Microfluidic Electromanipulation with Capacitive Detection for Cell Diagnostic Applications

G.A. Ferrier[*], A.N. Hladio[*], D.J. Thomson[*], G.E. Bridges[*],
M. Hedayatipoor[**], S. Olson[**], and M.R. Freeman[**]

[*]Department of Electrical and Computer Engineering, University of Manitoba, Winnipeg, Canada
gferrier@ee.umanitoba.ca
[**]Department of Physics and NINT, University of Alberta, Edmonton, Canada

ABSTRACT

We are proposing an approach to cell diagnostics that uses a combination of electromanipulation for stimulus and capacitance for sensing. The capacitance sensor consists of a 2 GHz cylindrical cavity resonator coupled to a pair of gold electrodes fabricated in a 25 x 100 x 120 μm^3 water-filled microfluidic channel. In this channel, the capacitance changes caused by the presence of yeast cells and polystyrene spheres were approximately 10 and 100 aF, respectively, with a capacitance resolution of 2 aF. These capacitance changes are in reasonable agreement with values provided by finite element simulations and the resolution is much better than that previously reported in the literature. We have trapped yeast cells by applying a 3 V, 1 MHz frequency signal and observed capacitance changes associated with the trapping and release of cells.

Keywords: capacitance sensor, cell diagnostics, microfluidics, dielectrophoresis, electromanipulation

1 INTRODUCTION

New directions of microfluidics research have resulted from the realization that mechanical responses of cells offer insight into many aspects of their behavior [1]. For single cells optical stretchers, micro-pipette aspiration, magnetic tweezers and micro-cantilevers are some of the approaches that have been explored [2]. Other groups have been successful in implementing high sensitivity electrical techniques for cell counting [3, 4, 5]. We are proposing an electrical approach to mechanical cell diagnostics that uses a combination of electromanipulation for stimulus and capacitance for sensing.

An all-electrical approach offers the possibility of rapid diagnostics and very high degrees of integration. Capacitive based sensing systems have been integrated into gyroscopes and have achieved 12 zF resolution [6]. If sensors of this sensitivity were combined with microfluidics systems for transporting cells, highly integrated diagnostic systems would be possible.

Electrical manipulation is possible because of the difference in the dielectric properties of cells and the surrounding fluid [7]. The dielectric difference in combination with electric field gradients can be used to translate or rotate cells [8]. The electric field itself can also be used to alter the shape of the cell through electrostatic pressure exerted on the cell [9]. Changes in both cell position and shape will result in changes in the capacitance between the electrodes that deliver the field.

In this work, high frequencies are used for capacitance detection. Using high frequency (GHz) signals avoids problems associated with electrical double layers at the electrode-fluid interface, which, at lower frequencies, can limit the capacitance resolution to 2 fF [3]. Finally, the use of high frequencies also opens the door for lower frequencies (MHz) to be used for other purposes such as the electromanipulation of materials as shown below.

2 CAPACITANCE SENSOR

The experimental apparatus for capacitance measurements is shown in Figure 1. An automated syringe pump delivers fluid and cells through a tube into the inlet connector of the microfluidic channel. Gold electrodes were fabricated across the channel at 90 degrees relative to the channel flow direction. To exploit the use of high frequencies in obtaining capacitance variations due to the presence of cells in the channel, a high-Q quarter wavelength cylindrical cavity resonator was brought into contact with the gold electrodes. The resonance frequency of the resonator is approximately 2 GHz. When the resonator contacts the gold electrodes, subsequent variations in the channel capacitance, such as the presence of cells, will vary the effective electrical length of the cavity resonator, and hence its resonance frequency.

We discern the resonance frequency by modulating the resonator drive frequency about the resonance frequency of the resonator-channel combination when the channel is filled with water or appropriate buffer solutions. When the resonator has a sufficiently high Q value, it is sensitive enough to monitor small capacitance variations [10]. Subsequent resonance shifts caused by cells passing by the sensing electrodes emerges as a difference between the signals at $f_r+\Delta f$ and $f_r-\Delta f$ (f_r and Δf are the resonant and modulation frequencies, respectively), which is monitored using a lock-in amplifier and oscilloscope. The response

NSTI-Nanotech 2007, www.nsti.org, ISBN 1420061836 Vol. 2, 2007

signal difference can be directly related to a capacitance change.

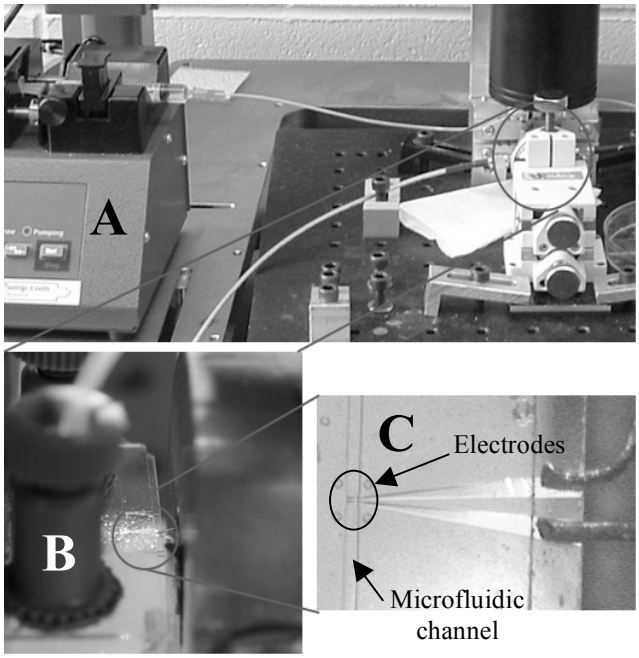

Figure 1: Experimental apparatus. An automated syringe pump (A) delivers water and cells through a tube into inlet connector (B) to the microfluidic channel (C).

3 EXPERIMENTAL RESULTS

Experimental results from polystyrene spheres and yeast cells in a water solution are provided in Figures 2 and 3, respectively. In both cases, we observe a decrease in capacitance because the permittivities of both polystyrene and yeast are less than that of water (80 ε_0). The larger capacitance change from polystyrene spheres (~ 100 aF) compared with yeast cells (~10 aF) occurs because the polystyrene spheres have a larger volume and a higher dielectric contrast compared with water. One can estimate the capacitance change using:

$$\Delta C = \frac{\left(\varepsilon_w - \varepsilon_{cell}\right) E^2 \left(Vol\right)}{V^2} \qquad (1)$$

where ε_w and ε_{cell} are the water and cell permittivities, E and V are the electric field and potential difference between the electrodes, and Vol is the particle volume. Capacitance differences within each figure arise because different particles pass at different heights above the electrode plane and due to particle size variations.

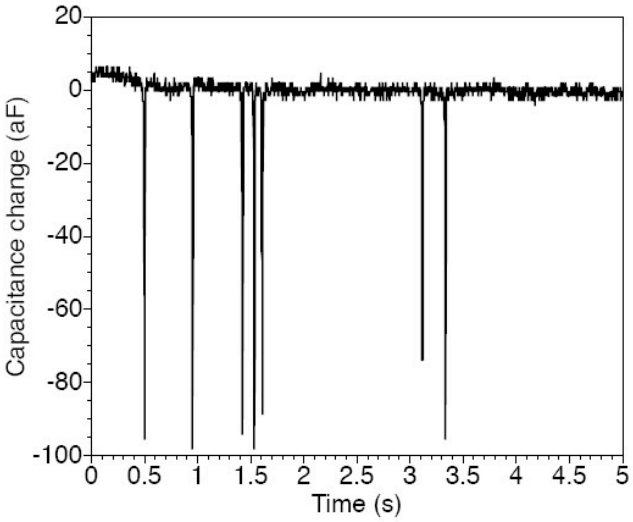

Figure 2: Capacitance changes caused by 10 μm polystyrene spheres.

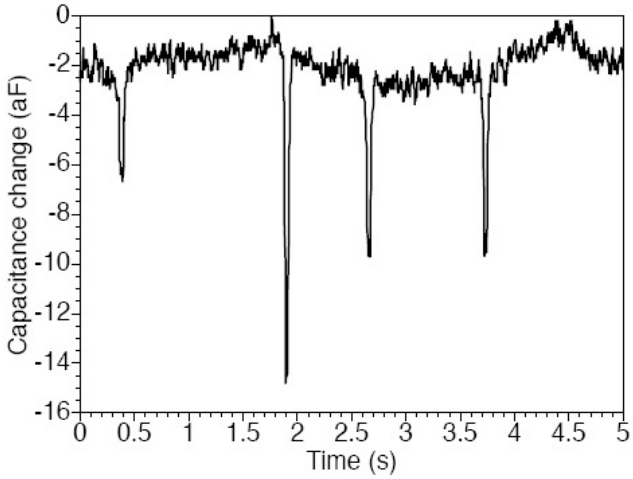

Figure 3: Capacitance changes caused by 6 μm yeast cells.

4 SIMULATIONS

Finite element analysis simulations were performed using the COMSOL® electromagnetics module. The Laplace equation, $\nabla^2 V = 0$, was used to solve for the electric fields in the channel. Since polystyrene spheres and yeast cells are simple model systems, they were modeled as single-shelled spheres having an effective permittivity given by [11]

$$\varepsilon_{cell} = \varepsilon_{memb} \left\{ \frac{a^3 + 2\left(\frac{\varepsilon_{cyt} - \varepsilon_{memb}}{\varepsilon_{cyt} + 2\varepsilon_{memb}}\right)}{a^3 - \left(\frac{\varepsilon_{cyt} - \varepsilon_{memb}}{\varepsilon_{cyt} + 2\varepsilon_{memb}}\right)} \right\}; \qquad a = \frac{R}{R-d},$$

where ε_{memb} and ε_{cyt} are the membrane and cytoplasm permittivities, R is the cell radius, and d is the membrane thickness. The values of these parameters for polystyrene and yeast are given in Table 1.

Material	$\varepsilon_{cytoplasm}$	$\varepsilon_{membrane}$	ε_{water}	Radius (μm)
Yeast	60	5	80	3
Polystyrene	2.5	N/A	80	5

Table 1: Permittivity and radius values of polystyrene spheres and yeast cells

Figures 4 and 5 show the simulated capacitance changes as a function of particle position for yeast cells and polystyrene spheres, respectively. Both the channel depth and the electrode spacing are 25 μm. The membrane permittivity was calculated using the parallel plate approximation, $C = \varepsilon A/d$, often used in the literature. For a typical membrane thickness of 5 nm and a membrane capacitance per unit area of 0.01 F/m^2 [12], the relative permittivity is about 5.

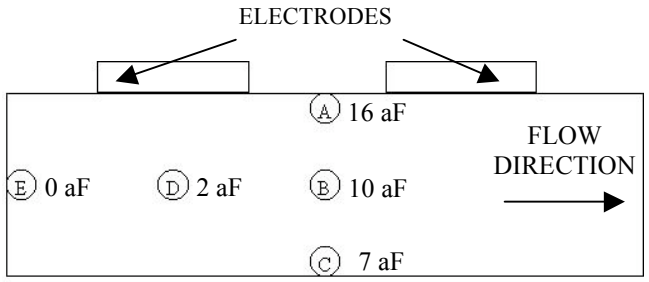

Figure 4: Capacitance change of 6 μm yeast cells as a function of position. A) 16 aF, B) 10 aF, C) 7 aF, D) 2 aF, and E) 0 aF. The electrode width and channel height are 25 μm each (not drawn to scale).

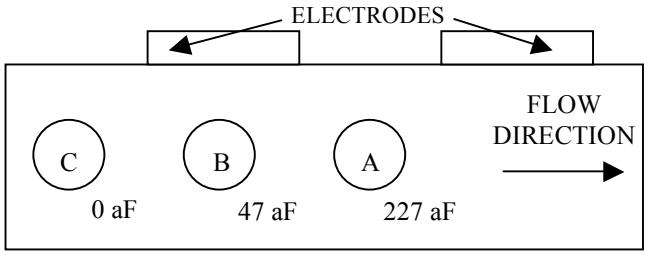

Figure 5: Capacitance change of 10 μm polystyrene spheres as a function of position. A) 227 aF, B) 47 aF, and C) 0 aF. The electrode width and channel height are 25 μm each (not drawn to scale).

The simulation results agree reasonably well with the experimental results, suggesting that the particles more or less remain on the same plane as that of maximum velocity. In laminar flow, which occurs almost exclusively in microfluidic systems, the velocity profile is parabolic, having a maximum in the center of the channel and zero at the channel edges. For the polystyrene case, the predicted capacitance change is approximately twice that of the experimental capacitance change. This is likely due to a larger dielectrophoresis force, which arises from the sphere having a larger volume. At high frequencies (2 GHz), this force will be repulsive, making the sphere flow through the channel at a lower vertical position, which would cause a smaller capacitance change. As expected, the simulation also predicts that the capacitance change has a relatively strong dependence on the vertical position of the cell relative to the electrodes.

5 DIELECTROPHORETIC TRAPPING

At frequencies of a few MHz, most cells exhibit an effective dielectric constant greater than water. By applying signals at 1-2 MHz, cells will be attracted to electrodes in water. If the applied voltage is high enough, 3 V or so in our case, the attractive forces will overcome the forces due to fluid flow and cells will become trapped on the electrodes. When the voltage is removed, the cells will be released. We have demonstrated this effect and have used the capacitive sensor to detect the trapping of these cells (Figure 6). This was the first demonstration of electromanipulation of cells with simultaneous capacitive detection in microfluidic channels.

Each voltage dip in Figure 6 represents an event, whether it is a cell passing by the electrode pair or the trapping of an individual cell. As yeast cells flowed through the channel, a 1 MHz trapping signal was turned on and off every 5 seconds. Giving particular attention to the 22-27 s timeframe in Figure 6, when the trapping signal was on, we observed the sequential trapping of three individual yeast cells. When the trapping signal was turned off at 27 s, the three trapped cells were released. These events were observed both optically and via capacitance detection. During those timeframes when the trapping signal was off, the smaller voltage dips correspond only to the flow of individual yeast cells by the electrode pair.

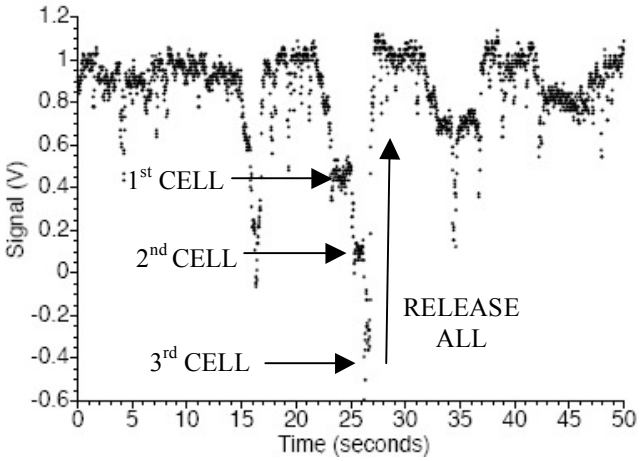

Figure 6: Periodic trapping and release of yeast cells.

NSTI-Nanotech 2007, www.nsti.org, ISBN 1420061836 Vol. 2, 2007

6 CONCLUSIONS

We have developed a system that can successfully detect the presence of yeast cells and polystyrene spheres with a 2 aF capacitance resolution. In addition, we have used capacitive detection for monitoring the dielectrophoretic trapping and release of flowing yeast cells. Preliminary dielectrophoretic force calculations indicate that the forces within the channel are in the pN range, which should make electrodeformation experiments feasible.

7 ACKNOWLEDGEMENTS

The authors wish to thank the National Institute for Nanotechnology (NINT), the Natural Sciences and Engineering Research Council (NSERC), the Canada Foundation for Innovation (CFI), the Canadian Institute for Advanced Research (CIAR) and Canada Research Chair for financial support of this research.

REFERENCES

[1] S. Suresh, J. Spatz, J.P. Mills, A. Micoulet, M. Dao, C.T. Lim, M. Beil, and T. Seufferlein, "Connections between single-cell biomechanics and human disease states: gastrointestinal cancer and malaria," Acta Biomaterialia, 1, 15-30, 2005.

[2] K.J. Van Vliet, G. Bao, and S. Suresh, "The biomechanics toolbox: experimental approaches for living cells and biomolecules," Acta Materialia, 51, 5881–5905, 2003.

[3] L.L. Sohn, O.A. Saleh, G.R. Facer, A.J. Beavis, R.S. Allan, and D.A. Notterman, "Capacitance cytometry: measuring biological cells one by one," Proc. Natl. Acad. Sci., 97(20), 10687-10690, 2000.

[4] S. Gawad, L. Schild, and Ph. Renaud, "Micromachined impedance spectroscopy flow cytometer for cell analysis and particle sizing," Lab on a Chip, 1, 76-82, 2001.

[5] D.K. Wood, S.-H. Oh, S.-H. Lee, H.T. Soh, and A.N. Cleland, "High bandwidth radio frequency Coulter counter," Applied Physics Letters, 87, 184106, 2005.

[6] J. A. Geen, S.J. Sherman, J.F. Chang, and S.R. Lewis, "Single-chip surface micromachined integrated gyroscope with 50°/h Allan deviation," IEEE Journal of Solid State Circuits, 37(12), 1860-1866, 2002.

[7] U. Zimmermann, U. Friedrich, H. Mussauer, P. Gessner, K. Hamel, and V. Sukhorukov, "Electromanipulation of mammalian cells: fundamentals and application," IEEE Transactions on Plasma Science, 28(1), 72-82, 2000.

[8] X-B. Wang, Y. Huang, R. Holzel, J.P.H. Burt, and R. Pethig, "Theoretical and experimental investigations of the interdependence of the dielectric, dielectrophoretic, and electrorotational behaviour of colloidal particles," J. Phys. D: Appl. Phys., 26, 312-322, 1993.

[9] T.L. Mahaworasilpa, "Cell electro-dynamics: the mechanics of living cells in intense alternating electric fields," Ph.D. Dissertation, Faculty of Science, The University of New South Wales, Australia, 1992.

[10] T. Tran, D.R. Oliver, D.J. Thomson and G.E. Bridges, "Zeptofarad (10^{-21} F) resolution capacitance sensor for scanning capacitance microscopy," Review of Scientific Instruments, 72(6), 2618-2623, 2001.

[11] T.B. Jones, "Electromechanics of particles." Cambridge University Press, New York, 1995.

[12] J. Gimsa, T. Müller, T. Schnelle, and G. Fuhr, "Dielectric spectroscopy of single human erythrocytes at physiological ionic strength: dispersion of the cytoplasm," Biophysical Journal, 71, 495-506, 1996.